Bull. Natl. Mus. Nat. Sci., Ser. C, 46, pp. 15–22, December 25, 2020

Depositional and metamorphic age estimations of low- *P/T* type Higo gneiss in the Amakusa-Kamishima Island, Kumamoto, southwest Japan

Yukiyasu Tsutsumi[1, 2]

[1] Department of Geology and Paleontology, National Museum of Nature and Science,
4–1–1 Amakubo, Tsukuba, Ibaraki 305–0005, Japan
[2] Faculty of Life and Environmental Sciences, University of Tsukuba,
1–1–1 Tennodai, Tsukuba, Ibaraki 305–8572, Japan
*Author for correspondence: ytsutsu@kahaku.go.jp

Abstract There are two major theories about the tectonics of the Higo Metamorphic Complex (HMC); with either Permo-Triassic or Early Cretaceous metamorphics. To clarify the ages of deposition and metamorphism, radiometric U-Pb ages of zircons in the gneiss of the HMC from Amakusa-Kamishima Island were obtained using a LA-ICP-MS. 146 measurements of core and mantle were obtained from 143 detrital zircon grains, of which 129 were concordant. The youngest age cluster (YC1σ) of detrital core and mantle has an age of 218.2 ± 2.9 Ma (1σ), which indicates the older limit of the depositional age of the protolith. The zircon grains in the sample have thin rims, and so only one datum could be obtained from the rim, which indicates an age of 116.0 ± 1.8 Ma (1σ). Considering these and previous data, the gneiss of the HMC was deposited after early Mesozoic and metamorphosed in the Early Cretaceous around 116 Ma.

Key words: zircon, U-Pb age, Early Cretaceous, detrital, metamorphic

Introduction

Several theories about the formation of the Higo belt has been proposed. However, nowadays there are two major theories which suggest the Higo belt is either a Permo-Triassic or Early Cretaceous igneous-metamorphic complex. Osanai *et al.* (2006) concluded that the Higo belt is a Permo-Triassic (ca. 250 Ma) metamorphic complex and the eastern extension of a collision zone between the North China and South China cratons. Late Triassic (ca. 211 Ma) and Cretaceous (ca. 120 Ma) granitoids then intruded after the metamorphism. Cretaceous ages reported from many locations in the Higo belt were thought to be the result of rejuvenescence due to the thermal effect from the later intrusions. On the other hand, zircon U-Pb age data suggest that the Higo belt is an Early Cretaceous igneous-metamorphic complex because the age of the granitoid and metamorphic rim of the gneiss indicate an Early Cretaceous age (Sakashima et al, 2003).

However, zircon U-Pb age data from the Higo belt is still poor. Therefore, the objective of this work is to add to the age data of the Higo gneiss. Population of detrital zircon core and metamorphic rim aged are provided in this paper.

Geological settings and sample

The Higo belt located in central Kyushu (Fig. 1) consists of various rock types; from north to south, the high -*P/T* type Manotani Metamorphic Complex, the low -*P/T* type Higo Metamorphic Complex (HMC), the Higo Plutonic Complex (HPC) and the low -*P/T* type Ryuhozan Metamorphic Complex (Yamamoto, 1962). The HPC and HMC extend west to the southeastern coast of Amakusa-Kamishima Island (Fig. 2).

The HMC is andalusite-sillimanite type metamorphic rocks which metamorphic grade increasing toward south to granulite facies (e.g. Yamamoto, 1962, 1983; Tsuji, 1967; Obata *et al.*, 1994; Osanai *et al.*, 1998; Maki et.al., 2004, 2009; Miyazaki, 2004). Biotite, muscovite and hornblende K-Ar and Rb-Sr ages of the HMC range from 97.9 ± 2.2 Ma to 109.8 ± 2.4 Ma (Hamamoto *et al.*, 1999; Nagakawa *et al.*, 1997; Nakajima *et al.*, 1995; Shibata and Yamamoto, 1965; Yamaguchi and Minamishin, 1986), most of which are concentrated in 101–107 Ma range. Sm-Nd whole rock-mineral isochron

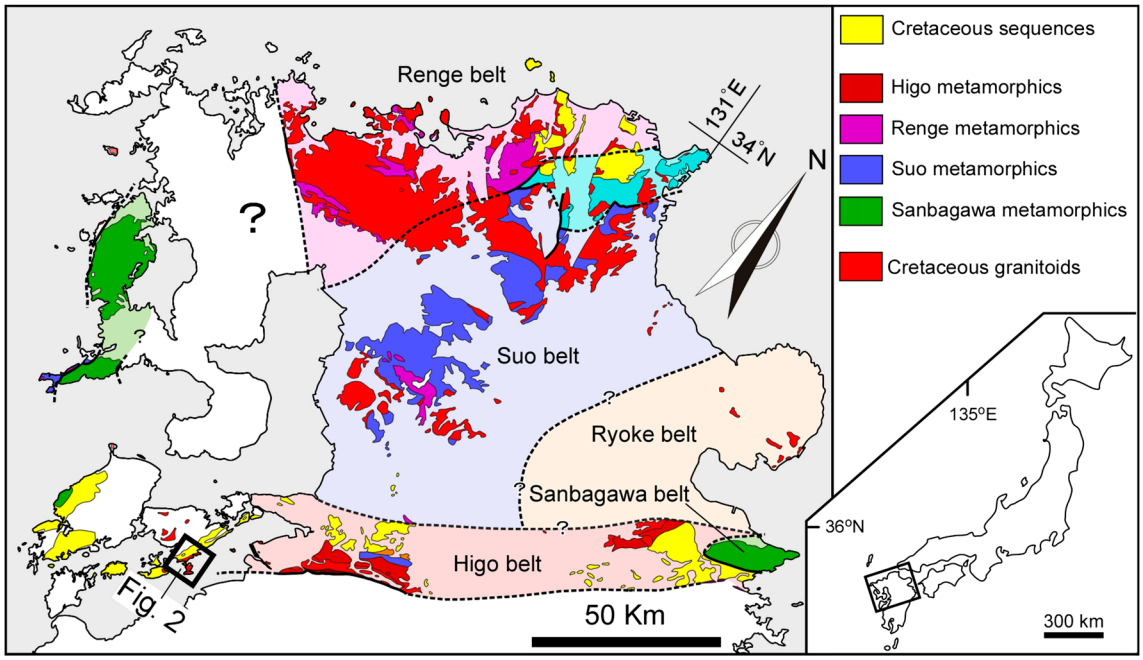

Fig. 1. Distribution map of the pre-Paleogene rocks in northern Kyushu.

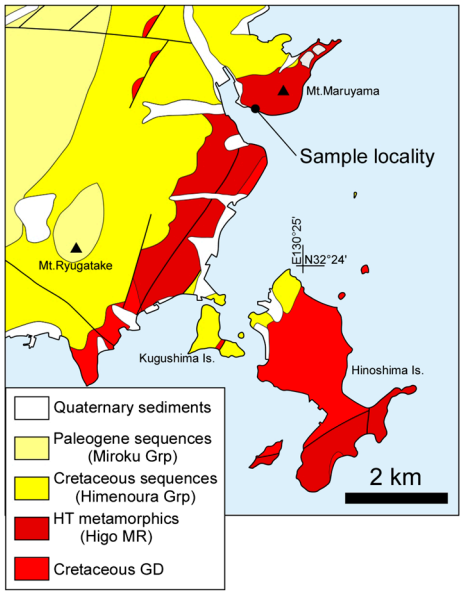

Fig. 2. Geological map showing the sampling localities modified after Hoshizumi *et al.* (2004).

and Rb-Sr whole rock ages range from 226.1 ± 28.4 Ma to 278.8 ± 4.9 Ma (Hamamoto *et al.*, 1999; Osanai *et al.*, 1993, 2001; Yamaguchi & Minamishin, 1986). Zircon U-Pb ages are reported from a paragneiss in the HMC; with detrital core ages of 160–330, 420, 1350 and 2160 Ma, and with a weighted mean age of metamorphic rims with low Th/U of 116.5 ± 18.7 Ma (95% conf.; Sakashima *et al.*, 2003). Two types of migmatites are present in the southern part of the HMC; metatexite and diatexite. Zircon grains in the metatexite have overgrowth rims with low Th/U and weighted mean age of the rim of 116.0 ± 1.6 Ma, whereas zircon grains in the diatexite have no overgrowth rims and a weighted mean age of 110.1 ± 0.6 Ma (95% conf.; Maki *et al.*, 2014).

The sample used is garnet-biotite gneiss of the HMC collected from south of Mt. Maruyama in the southeastern part of Amakusa-Kamishima Island (lat: 32°25′21.80″N, long: 130°24′30.50″E). The sample is stored in the National Museum of Nature and Science and has registration number NSM-R-134652.

Analytical methods

Before separation of zircon grains, the rock samples were scrubbed, and washed in an ultrasonic bath for ten minutes to avoid possible zircon contaminants. The zircon grains were handpicked from heavy fractions that were separated from the rock samples by standard crushing and heavy-liquid techniques. Zircon grains from the samples, the zircon standards FC1 (1099 Ma; Paces and Miller, 1993) and OT-4 (191.1 Ma; Horie *et al.*, 2013), and the glass standard NIST SRM610 were mounted in an epoxy resin and polished till the center of the embedded grains exposed on the surface. Backscattered electron and cathodoluminescence images of zircon grains were taken using a scanning electron

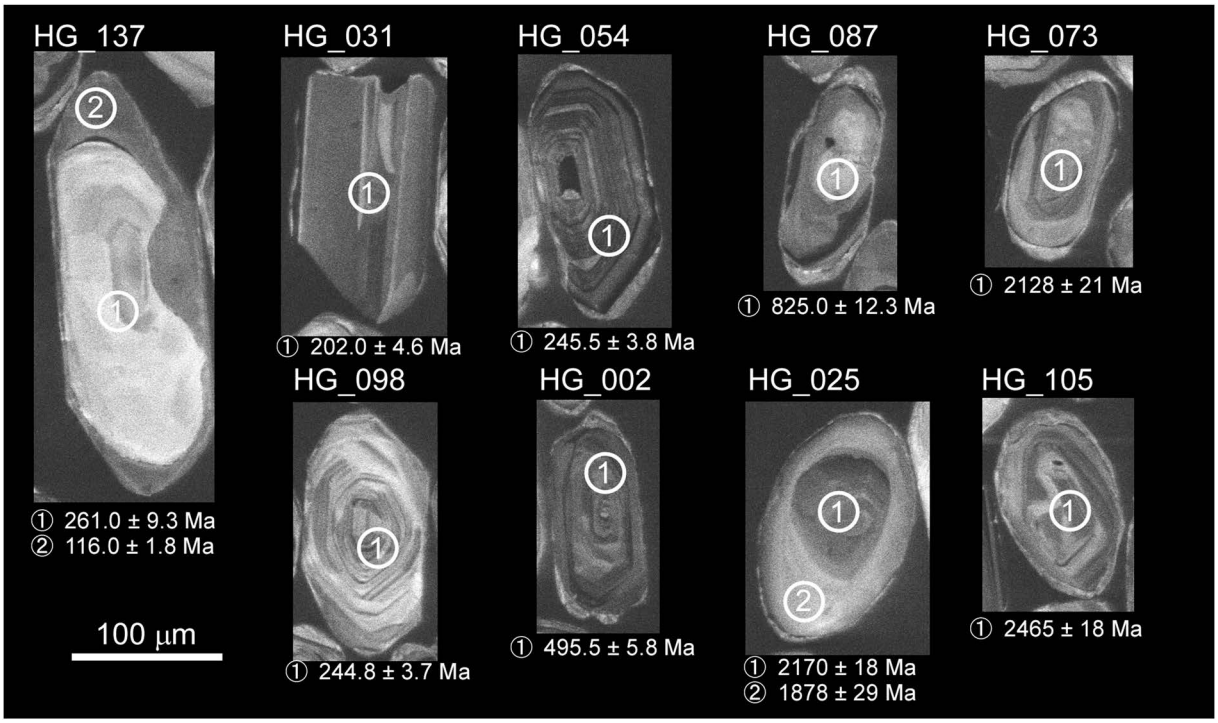

Fig. 3. Cathodoluminescence (CL) image of typical zircon grains. Circles on the images point to analyzed spots by LA-ICP-MS, of which diameter are 25 μm approx.

microscope-cathodoluminescence (SEM-CL) equipment, JSM-6610 (JEOL) and a CL detector (SANYU electron), installed at National Museum of Nature and Science, Japan. The images were applied to select the sites for analysis. U-Pb dating of these samples was carried out using LA-ICP-MS that was composed of NWR213 (Elemental Scientific Lasers) and Agilent 7700x (Agilent Technologies) installed at National Museum of Nature and Science, Japan. The experimental conditions and the analytical procedures followed for the measurements were after Tsutsumi *et al.* (2012). The spot size of the laser was 25 μm. A correction for common Pb was made on the basis of the measured $^{208}Pb/^{206}Pb$ and Th/U ratios (^{208}Pb correction) (e.g. Williams, 1998) and the model for common Pb compositions proposed by Stacey and Kramers (1975). $^{206}Pb^*$ indicates radiometric ^{206}Pb. The data of secondary standard OT-4 zircon obtained during analysis yielded a weighted mean age of 190.1 ± 1.9 Ma (95% conf.; n = 10; MSWD = 0.41). MSWD is acronym of mean square weighted deviation, which is calculated from square root of chi-square value.

Results

Almost all the zircon grains in the sample have thin rim and most of the cores have igneous zonings on the BSE and/or CL images (Fig. 3). Table 1 lists zircon data in terms of the fraction of common ^{206}Pb, U and Th concentrations, Th/U, $^{238}U/^{206}Pb^*$ and $^{207}Pb^*/^{206}Pb^*$ ratios, and radiometric $^{238}U/^{206}Pb^*$ ages of the sample. All errors are 1σ. 147 spots were analyzed in 143 grains. Only one concordant datum was collected from the rim (HG_137.2) and the remaining 146 data were from core or mantle. Among the core or mantle data, 129 data are concordant. The criteria of concordant is for 2σ overlap of the concordia curve on a concordia diagram (U-Pb age < 1000 Ma) and discordancy (Song *et al.*, 1996) of less than 15% (U-Pb age ≥ 1000 Ma). The $^{207}Pb^*/^{206}Pb^*$ age is applied when the age is ≥ 1000 Ma. The Th/U ratio of the zircon rim is lower than that of the zircon cores and mantles. These data show that most of the cores and mantles are igneous (detrital) in origin whereas the rims are metamorphic in origin (Williams and Claesson, 1987; Schiøtte *et al.*, 1988; Kinny *et al.*, 1990; Hoskin & Black, 2000). Figures 4 and 5 show Tera–Wasserberg concordia diagrams for all analyzed spots and the probability distribution diagram with

Table 1. LA-ICP-MS U-Pb data and calculated ages

Labels	$^{206}Pb_c$(1) (%)	U (ppm)	Th (ppm)	Th/U	$^{238}U/^{206}Pb^*$(1)	$^{207}Pb^*/^{206}Pb^*$(1)	$^{238}U/^{206}Pb^*$ age(1) (Ma)	$^{207}Pb^*/^{206}Pb^*$ age(1) (Ma)	Disc(2) (%)	Remarks
HG_001.1	0.64	237	136	0.59	3.46 ± 0.04	0.1083 ± 0.0018	1635.0 ± 18.4	1772 ± 30	7.73	
HG_002.1	0.09	997	149	0.15	12.52 ± 0.15	0.0580 ± 0.0010	495.5 ± 5.8			
HG_003.1	0.00	459	645	1.44	20.77 ± 0.30	0.0553 ± 0.0015	303.1 ± 4.3			
HG_004.1	0.10	133	4	0.03	2.66 ± 0.04	0.1693 ± 0.0022	2056.0 ± 24.3	2552 ± 22	19.44	discordant
HG_005.1	0.00	240	33	0.14	3.77 ± 0.05	0.1149 ± 0.0015	1518.3 ± 18.9	1879 ± 23	19.20	discordant
HG_006.1	0.00	197	87	0.45	23.48 ± 0.39	0.0504 ± 0.0021	268.8 ± 4.3			
HG_007.1	0.41	903	328	0.37	3.43 ± 0.05	0.1300 ± 0.0013	1650.2 ± 19.7	2099 ± 17	21.38	discordant
HG_008.1	1.18	395	322	0.84	2.48 ± 0.05	0.1471 ± 0.0042	2182.4 ± 37.5	2313 ± 49	5.65	
HG_008.2	0.00	369	43	0.12	3.67 ± 0.06	0.1153 ± 0.0014	1554.7 ± 21.9	1886 ± 21	17.57	discordant
HG_009.1	0.00	126	60	0.49	23.61 ± 0.44	0.0550 ± 0.0029	267.4 ± 4.9			
HG_010.1	0.00	252	58	0.24	3.55 ± 0.05	0.1156 ± 0.0011	1601.8 ± 19.2	1891 ± 17	15.29	discordant
HG_011.1	0.00	266	36	0.14	3.63 ± 0.05	0.1169 ± 0.0015	1569.2 ± 18.2	1910 ± 23	17.84	discordant
HG_012.1	0.01	504	384	0.78	25.45 ± 0.36	0.0546 ± 0.0033	248.4 ± 3.5			
HG_013.1	0.00	454	75	0.17	3.43 ± 0.04	0.1147 ± 0.0012	1649.0 ± 17.4	1877 ± 18	12.14	
HG_014.1	2.66	290	222	0.78	24.85 ± 0.46	0.0549 ± 0.0047	254.3 ± 4.6			
HG_015.1	0.22	97	89	0.95	3.10 ± 0.05	0.1131 ± 0.0033	1801.3 ± 25.8	1852 ± 52	2.74	
HG_016.1	0.00	792	700	0.91	2.42 ± 0.03	0.1617 ± 0.0013	2228.6 ± 21.9	2475 ± 14	9.95	
HG_017.1	0.00	232	108	0.48	3.29 ± 0.05	0.1138 ± 0.0014	1709.9 ± 21.8	1862 ± 23	8.17	
HG_017.2	0.00	302	185	0.63	3.39 ± 0.04	0.1146 ± 0.0012	1664.5 ± 17.6	1875 ± 19	11.23	
HG_018.1	0.00	396	311	0.81	27.31 ± 0.36	0.0518 ± 0.0015	231.8 ± 3.0			
HG_019.1	0.00	130	63	0.50	24.41 ± 0.51	0.0547 ± 0.0033	258.8 ± 5.3			
HG_020.1	0.33	114	85	0.77	25.68 ± 0.51	0.0512 ± 0.0058	246.2 ± 4.8			
HG_021.1	0.00	758	31	0.04	4.19 ± 0.06	0.1103 ± 0.0011	1378.8 ± 17.6	1805 ± 18	23.61	discordant
HG_022.1	0.10	121	67	0.57	24.03 ± 0.52	0.0556 ± 0.0051	262.8 ± 5.5			
HG_023.1	0.00	400	70	0.18	3.13 ± 0.04	0.1125 ± 0.0013	1787.6 ± 21.6	1841 ± 20	2.90	
HG_024.1	0.93	241	143	0.61	20.91 ± 0.36	0.0479 ± 0.0041	301.2 ± 5.1			
HG_025.1	0.00	390	224	0.59	2.99 ± 0.05	0.1353 ± 0.0015	1861.2 ± 24.9	2170 ± 18	14.23	
HG_025.2	0.11	220	41	0.19	3.47 ± 0.05	0.1148 ± 0.0018	1632.9 ± 19.5	1878 ± 29	13.05	
HG_026.1	1.39	380	164	0.44	4.01 ± 0.06	0.0996 ± 0.0028	1435.5 ± 18.9	1618 ± 51	11.28	
HG_027.1	0.00	680	71	0.11	3.45 ± 0.05	0.1145 ± 0.0013	1640.8 ± 19.8	1874 ± 21	12.44	
HG_028.1	0.00	122	44	0.37	27.18 ± 0.57	0.0583 ± 0.0032	233.0 ± 4.8			discordant
HG_029.1	0.00	563	73	0.13	28.07 ± 0.39	0.0503 ± 0.0014	225.7 ± 3.1			
HG_030.1	0.49	532	386	0.74	3.56 ± 0.06	0.1108 ± 0.0038	1597.1 ± 23.8	1813 ± 62	11.91	
HG_031.1	1.09	405	170	0.43	31.42 ± 0.73	0.0453 ± 0.0032	202.0 ± 4.6			
HG_032.1	0.00	96	49	0.52	27.48 ± 0.67	0.0552 ± 0.0034	230.4 ± 5.5			
HG_033.1	0.00	465	273	0.60	26.12 ± 0.40	0.0509 ± 0.0018	242.2 ± 3.7			
HG_034.1	0.00	58	25	0.45	28.07 ± 0.80	0.0573 ± 0.0053	225.6 ± 6.3			
HG_035.1	0.00	432	367	0.87	13.94 ± 0.22	0.0559 ± 0.0015	446.7 ± 6.7			
HG_036.1	0.00	77	55	0.73	24.93 ± 0.61	0.0503 ± 0.0036	253.5 ± 6.1			
HG_037.1	0.25	308	249	0.83	23.07 ± 0.37	0.0496 ± 0.0035	273.5 ± 4.3			
HG_038.1	0.03	233	121	0.53	13.35 ± 0.21	0.0568 ± 0.0026	465.5 ± 7.0			
HG_039.1	0.00	253	155	0.63	24.86 ± 0.40	0.0512 ± 0.0021	254.2 ± 4.0			
HG_040.1	0.13	236	157	0.68	26.24 ± 0.49	0.0500 ± 0.0044	241.1 ± 4.4			
HG_041.1	0.00	923	1250	1.39	3.29 ± 0.04	0.1158 ± 0.0011	1712.8 ± 19.7	1893 ± 17	9.52	
HG_042.1	0.48	269	112	0.43	3.55 ± 0.06	0.1124 ± 0.0020	1601.2 ± 23.6	1839 ± 32	12.93	
HG_043.1	0.00	591	264	0.46	25.47 ± 0.38	0.0506 ± 0.0013	248.2 ± 3.6			
HG_044.1	0.00	250	98	0.40	3.21 ± 0.04	0.1128 ± 0.0015	1747.1 ± 21.4	1847 ± 23	5.41	
HG_045.1	0.00	326	104	0.33	3.41 ± 0.05	0.1132 ± 0.0013	1659.7 ± 21.4	1852 ± 21	10.38	
HG_046.1	0.00	591	247	0.43	26.18 ± 0.40	0.0492 ± 0.0011	241.6 ± 3.6			
HG_047.1	0.00	33	12	0.37	19.44 ± 0.54	0.0548 ± 0.0055	323.4 ± 8.8			
HG_048.1	0.00	763	426	0.57	26.38 ± 0.35	0.0503 ± 0.0014	239.8 ± 3.1			
HG_049.1	0.13	235	58	0.25	3.24 ± 0.04	0.1240 ± 0.0020	1734.9 ± 19.9	2016 ± 28	13.94	
HG_050.1	0.47	145	67	0.48	25.74 ± 0.58	0.0487 ± 0.0054	245.7 ± 5.4			
HG_051.1	0.31	211	58	0.28	3.58 ± 0.05	0.1135 ± 0.0025	1589.4 ± 20.9	1858 ± 39	14.46	
HG_052.1	0.00	90	46	0.53	23.00 ± 0.57	0.0508 ± 0.0042	274.4 ± 6.6			
HG_053.1	0.00	352	231	0.67	3.16 ± 0.05	0.1157 ± 0.0015	1770.3 ± 22.8	1892 ± 23	6.43	
HG_054.1	0.29	1472	881	0.61	25.76 ± 0.40	0.0492 ± 0.0022	245.5 ± 3.8			
HG_055.1	0.00	1305	884	0.69	24.47 ± 0.37	0.0530 ± 0.0012	258.2 ± 3.8			
HG_056.1	0.66	81	40	0.51	22.98 ± 0.62	0.0459 ± 0.0072	274.6 ± 7.2			
HG_057.1	0.77	447	386	0.89	23.90 ± 0.46	0.0432 ± 0.0050	264.2 ± 4.9			
HG_058.1	0.00	365	171	0.48	2.22 ± 0.03	0.1717 ± 0.0015	2398.1 ± 28.1	2576 ± 14	6.91	
HG_059.1	0.03	733	154	0.22	25.15 ± 0.38	0.0520 ± 0.0017	251.3 ± 3.7			
HG_060.1	0.00	192	98	0.52	25.46 ± 0.52	0.0539 ± 0.0027	248.4 ± 5.0			
HG_061.1	0.00	171	84	0.50	25.66 ± 0.49	0.0545 ± 0.0026	246.4 ± 4.6			
HG_062.1	0.00	387	534	1.41	25.08 ± 0.44	0.0534 ± 0.0020	252.0 ± 4.4			
HG_063.1	0.00	281	166	0.61	25.21 ± 0.45	0.0513 ± 0.0018	250.8 ± 4.4			
HG_064.1	0.76	361	284	0.81	24.71 ± 0.44	0.0485 ± 0.0045	255.7 ± 4.4			
HG_065.1	0.00	448	130	0.30	3.22 ± 0.04	0.1128 ± 0.0012	1742.2 ± 21.3	1847 ± 18	5.67	
HG_066.1	0.00	217	93	0.44	3.45 ± 0.05	0.1138 ± 0.0014	1639.6 ± 21.3	1862 ± 22	11.94	
HG_067.1	0.00	215	117	0.56	3.24 ± 0.04	0.1148 ± 0.0015	1732.3 ± 20.7	1878 ± 23	7.76	
HG_068.1	8.46	227	105	0.47	25.90 ± 0.55	0.0606 ± 0.0111	244.2 ± 5.1			
HG_069.1	0.08	90	60	0.69	13.19 ± 0.27	0.0574 ± 0.0051	471.0 ± 9.4			
HG_070.1	0.00	254	69	0.28	3.47 ± 0.05	0.1158 ± 0.0016	1630.5 ± 22.8	1894 ± 24	13.91	
HG_071.1	0.00	329	354	1.11	3.24 ± 0.05	0.1183 ± 0.0017	1735.1 ± 22.3	1931 ± 26	10.14	
HG_072.1	0.09	664	493	0.76	27.68 ± 0.45	0.0504 ± 0.0030	228.8 ± 3.7			
HG_073.1	0.00	466	244	0.54	2.77 ± 0.04	0.1322 ± 0.0015	1988.5 ± 24.8	2128 ± 21	6.55	

Table 1. Continued

Labels	$^{206}Pb_c$(1) (%)	U (ppm)	Th (ppm)	Th/U	$^{238}U/^{206}Pb^*$(1)	$^{207}Pb^*/^{206}Pb^*$(1)	$^{238}U/^{206}Pb^*$ age(1) (Ma)	$^{207}Pb^*/^{206}Pb^*$ age(1) (Ma)	Disc(2) (%)	Remarks
HG_074.1	0.04	992	432	0.45	25.15 ± 0.45	0.0521 ± 0.0019	251.4 ± 4.4			
HG_075.1	0.00	572	320	0.57	25.27 ± 0.36	0.0510 ± 0.0015	250.2 ± 3.5			
HG_076.1	2.78	115	55	0.49	3.72 ± 0.06	0.1216 ± 0.0036	1535.7 ± 22.1	1981 ± 51	22.48	discordant
HG_077.1	0.27	100	80	0.82	26.12 ± 0.72	0.0517 ± 0.0072	242.2 ± 6.6			
HG_078.1	0.00	271	204	0.77	2.40 ± 0.04	0.1640 ± 0.0018	2244.7 ± 28.9	2498 ± 19	10.14	
HG_079.1	0.39	556	304	0.56	24.17 ± 0.41	0.0529 ± 0.0028	261.3 ± 4.3			
HG_080.1	1.13	371	193	0.53	14.03 ± 0.25	0.0548 ± 0.0027	443.9 ± 7.6			
HG_081.1	0.25	394	121	0.32	3.33 ± 0.05	0.1120 ± 0.0020	1694.2 ± 22.5	1832 ± 33	7.52	
HG_082.1	0.28	381	133	0.36	13.55 ± 0.21	0.0551 ± 0.0020	459.0 ± 6.9			
HG_083.1	0.59	329	115	0.36	26.25 ± 0.45	0.0482 ± 0.0027	241.0 ± 4.1			
HG_084.1	0.50	262	116	0.46	25.28 ± 0.46	0.0476 ± 0.0031	250.1 ± 4.4			
HG_085.1	0.20	395	237	0.62	24.50 ± 0.40	0.0512 ± 0.0031	257.9 ± 4.1			
HG_086.1	0.08	316	56	0.18	3.36 ± 0.05	0.1182 ± 0.0015	1679.1 ± 21.9	1930 ± 22	13.00	
HG_087.1	0.13	228	76	0.34	7.32 ± 0.12	0.0697 ± 0.0020	825.0 ± 12.3			
HG_088.1	0.07	168	54	0.33	3.32 ± 0.05	0.1150 ± 0.0022	1698.3 ± 24.3	1881 ± 34	9.71	
HG_089.1	0.24	263	81	0.32	22.61 ± 0.45	0.0497 ± 0.0025	279.0 ± 5.4			
HG_090.1	0.00	157	76	0.50	25.53 ± 0.54	0.0559 ± 0.0024	247.7 ± 5.2			discordant
HG_091.1	0.44	787	388	0.51	26.83 ± 0.41	0.0504 ± 0.0022	235.9 ± 3.6			
HG_092.1	0.01	382	114	0.31	12.47 ± 0.17	0.0578 ± 0.0018	497.4 ± 6.6			
HG_093.1	0.00	738	264	0.37	26.27 ± 0.39	0.0512 ± 0.0015	240.8 ± 3.5			
HG_094.1	0.28	442	245	0.57	26.47 ± 0.44	0.0490 ± 0.0031	239.1 ± 3.9			
HG_095.1	0.13	765	48	0.06	13.85 ± 0.20	0.0582 ± 0.0011	449.5 ± 6.3			
HG_096.1	0.03	333	128	0.39	3.20 ± 0.04	0.1150 ± 0.0015	1751.1 ± 20.9	1881 ± 24	6.90	
HG_097.1	0.22	773	233	0.31	14.91 ± 0.21	0.0552 ± 0.0015	418.5 ± 5.6			
HG_098.1	0.00	292	166	0.58	25.84 ± 0.40	0.0485 ± 0.0019	244.8 ± 3.7			
HG_099.1	0.00	570	221	0.40	2.32 ± 0.03	0.1660 ± 0.0016	2308.8 ± 25.2	2519 ± 16	8.35	
HG_100.1	0.00	277	70	0.26	3.32 ± 0.05	0.1101 ± 0.0014	1695.4 ± 21.3	1802 ± 23	5.91	
HG_101.1	0.19	587	202	0.35	3.65 ± 0.04	0.1112 ± 0.0015	1561.5 ± 16.1	1820 ± 24	14.21	
HG_102.1	0.15	622	62	0.10	3.77 ± 0.05	0.1138 ± 0.0013	1517.9 ± 16.7	1862 ± 20	18.48	discordant
HG_103.1	0.07	102	63	0.64	25.41 ± 0.58	0.0576 ± 0.0063	248.8 ± 5.5			
HG_104.1	0.16	412	48	0.12	12.60 ± 0.21	0.0547 ± 0.0019	492.4 ± 7.8			
HG_105.1	0.00	287	338	1.21	2.20 ± 0.03	0.1608 ± 0.0017	2419.9 ± 30.2	2465 ± 18	1.83	
HG_106.1	0.00	1922	985	0.53	25.66 ± 0.34	0.0526 ± 0.0009	246.5 ± 3.2			
HG_107.1	0.00	795	725	0.94	22.10 ± 0.36	0.0525 ± 0.0010	285.3 ± 4.5			
HG_108.1	0.32	931	773	0.85	22.65 ± 0.43	0.0569 ± 0.0067	278.6 ± 5.2			
HG_109.1	0.00	236	47	0.20	3.19 ± 0.05	0.1126 ± 0.0015	1757.7 ± 23.3	1843 ± 23	4.63	
HG_110.1	0.00	270	89	0.34	24.31 ± 0.45	0.0508 ± 0.0018	259.9 ± 4.7			
HG_111.1	0.69	695	532	0.79	3.47 ± 0.06	0.1071 ± 0.0021	1634.3 ± 25.6	1751 ± 36	6.66	
HG_112.1	0.28	386	87	0.23	3.01 ± 0.04	0.1121 ± 0.0014	1847.3 ± 23.2	1834 ± 22	− 0.73	
HG_113.1	0.00	764	504	0.68	23.47 ± 0.36	0.0501 ± 0.0010	269.0 ± 4.1			
HG_114.1	0.47	652	207	0.33	24.10 ± 0.38	0.0506 ± 0.0019	262.0 ± 4.0			
HG_115.1	0.00	201	257	1.31	2.12 ± 0.03	0.1616 ± 0.0019	2493.4 ± 28.5	2474 ± 19	− 0.79	
HG_116.1	0.09	329	79	0.25	3.52 ± 0.05	0.1135 ± 0.0014	1611.5 ± 21.9	1857 ± 23	13.22	
HG_117.1	0.00	715	1225	1.76	26.45 ± 0.36	0.0495 ± 0.0012	239.2 ± 3.2			
HG_118.1	0.24	264	46	0.18	3.90 ± 0.05	0.1105 ± 0.0018	1472.2 ± 18.5	1809 ± 29	18.62	discordant
HG_119.1	0.00	149	62	0.42	22.71 ± 0.43	0.0548 ± 0.0026	277.8 ± 5.1			
HG_120.1	0.47	1424	797	0.57	29.33 ± 0.46	0.0502 ± 0.0020	216.1 ± 3.3			
HG_121.1	0.00	293	66	0.23	3.30 ± 0.04	0.1121 ± 0.0012	1706.4 ± 19.8	1836 ± 19	7.06	
HG_122.1	0.00	434	197	0.47	24.47 ± 0.36	0.0532 ± 0.0015	258.2 ± 3.8			
HG_123.1	0.00	230	177	0.79	25.88 ± 0.45	0.0527 ± 0.0023	244.4 ± 4.2			
HG_124.1	0.00	687	266	0.40	25.37 ± 0.34	0.0515 ± 0.0011	249.2 ± 3.2			
HG_125.1	0.00	651	430	0.68	3.24 ± 0.04	0.1197 ± 0.0011	1732.8 ± 19.0	1952 ± 17	11.23	
HG_126.1	0.00	61	37	0.63	23.95 ± 0.75	0.0495 ± 0.0052	263.7 ± 8.1			
HG_127.1	0.00	386	312	0.83	25.34 ± 0.42	0.0526 ± 0.0017	249.5 ± 4.1			
HG_128.1	0.00	630	440	0.72	25.97 ± 0.39	0.0549 ± 0.0012	243.5 ± 3.6			discordant
HG_129.1	0.32	114	58	0.52	26.57 ± 0.57	0.0569 ± 0.0064	238.1 ± 5.1			
HG_130.1	0.00	180	136	0.78	23.27 ± 0.42	0.0519 ± 0.0026	271.2 ± 4.8			
HG_131.1	0.00	223	101	0.46	23.16 ± 0.35	0.0528 ± 0.0021	272.4 ± 4.1			
HG_132.1	0.13	407	287	0.72	3.20 ± 0.05	0.1133 ± 0.0020	1754.0 ± 22.6	1855 ± 31	5.45	
HG_133.1	0.00	212	131	0.63	23.36 ± 0.39	0.0520 ± 0.0020	270.2 ± 4.4			
HG_134.1	0.00	140	109	0.80	2.73 ± 0.04	0.1688 ± 0.0020	2009.5 ± 25.0	2547 ± 20	21.10	discordant
HG_135.1	0.00	382	168	0.45	3.51 ± 0.05	0.1173 ± 0.0013	1615.0 ± 19.6	1917 ± 19	15.75	discordant
HG_136.1	0.00	526	478	0.93	24.56 ± 0.35	0.0530 ± 0.0013	257.3 ± 3.6			
HG_137.1	0.70	33	8	0.25	24.20 ± 0.88	0.0511 ± 0.0082	261.0 ± 9.3			
HG_137.2	0.04	593	6	0.01	55.09 ± 0.86	0.0502 ± 0.0023	116.0 ± 1.8			rim
HG_138.1	0.00	285	46	0.16	4.54 ± 0.07	0.1120 ± 0.0015	1283.2 ± 17.1	1834 ± 24	30.03	discordant
HG_139.1	0.25	412	137	0.34	13.07 ± 0.18	0.0564 ± 0.0018	475.4 ± 6.4			
HG_140.1	0.00	643	307	0.49	26.08 ± 0.43	0.0522 ± 0.0013	242.6 ± 3.9			
HG_141.1	0.00	460	61	0.14	3.54 ± 0.05	0.1166 ± 0.0012	1605.8 ± 19.3	1906 ± 19	15.75	discordant
HG_142.1	0.23	188	120	0.65	24.93 ± 0.48	0.0530 ± 0.0043	253.5 ± 4.8			
HG_143.1	0.00	111	21	0.20	13.46 ± 0.25	0.0554 ± 0.0020	462.1 ± 8.1			

Errors are 1-sigma; Pb_c and Pb* indicate the common and radiogenic portions, respectively.

(1) Common Pb corrected by assuming $^{206}Pb/^{238}U$-$^{208}Pb/^{232}Th$ age-concordance

(2) The degree of discordance for an analyzed spot indicates the chronological difference between the two ages determined by Pb-Pb and U-Pb methods, and is defined as $\{1 - (^{238}U/^{206}Pb^*\text{ age})/(^{207}Pb^*/^{206}Pb^*\text{ age})\} \times 100$ (%) (e.g., Song *et al.*, 1996).

histogram for the concordant ages of the zircon cores, respectively.

The concordant age data from the zircon cores and mantles form some clusters in the range of about 202 to 323 Ma (72 data), 418 to 497 Ma (12 data), 825 Ma (1 datum), 1618 to 2170 (37 data) and 2313 to 2576 Ma (7 data) (Fig. 5). The youngest single age (YSG) and weigthed mean of youngest cluster of more than 2 grain ages that overlap in age within 1σ (YC1σ) of core and mantle data are 202.0 ± 4.6 Ma (HG_031.1) and 218.2 ± 2.9 Ma (n = 2, MSWD = 1.80), respectively (Dickinson and Gehrels, 2009).

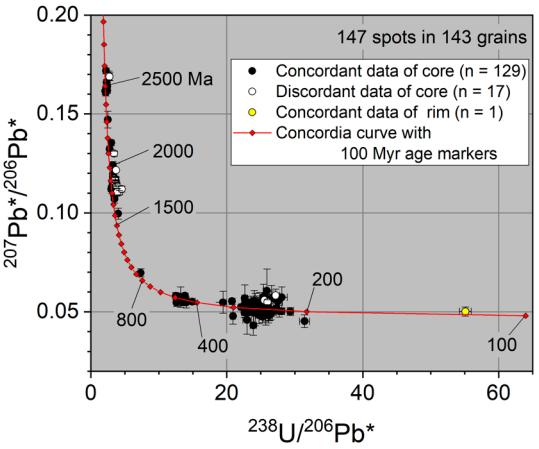

Fig. 4. Tera–Wasserburg U-Pb concordia diagrams of zircons in the sample. $^{207}Pb^*$ and $^{206}Pb^*$ indicate radiometric ^{207}Pb and ^{206}Pb, respectively. Solid curve indicates the concordia curve.

Discussion

In principle, YSG should indicate the older limit of the depositional age, but estimation based on multiple grain ages are generally more consistent (Dickinson and Gehrels, 2009). Therefore, YC1σ is better than YSG to indicate the older limit of the depositional age. The YC1σ of the core and mantle ages of 218.2 ± 2.9 (1σ) show that the protolith of the sample was deposited in or after Late Triassic. Moreover, the YC1σ calculated from concordant core age data reported by Sakashima *et al.* (2003) is 193.0 ± 5.4 Ma (1σ, n = 5, MSWD = 0.43) (Early Jurassic), which is younger than the data in this study. The older limit of depositional ages of the HMC are younger than the ages of metamorphism in the collision zone between the North China and South China cratons; UHP metamorphism in Qinling-Dabie-Sulu area in central China (~230 Ma; e.g. Hacker *et al.*, 1998; Chen *et al.*, 2003; Liu *et al.*, 2006; Wu *et al.*, 2008), medium -P/T type metamorphism in Imjingang belt in central Korian Peninsula (253 ± 2 Ma; Cho *et al.*, 2007) and in Unazuki metamorphics in central Japan (258–253 Ma; Horie *et al.*, 2018). Because metamorphism does not precede deposition, The HMC never suffered metamorphism related to the collision of the North China and South China cratons.

Only one spot datum, with the age of 116.0 ± 1.8 Ma (1σ), was obtained from a rim with a low Th/U ratio. However, Sakashma *et al.*, (2003)

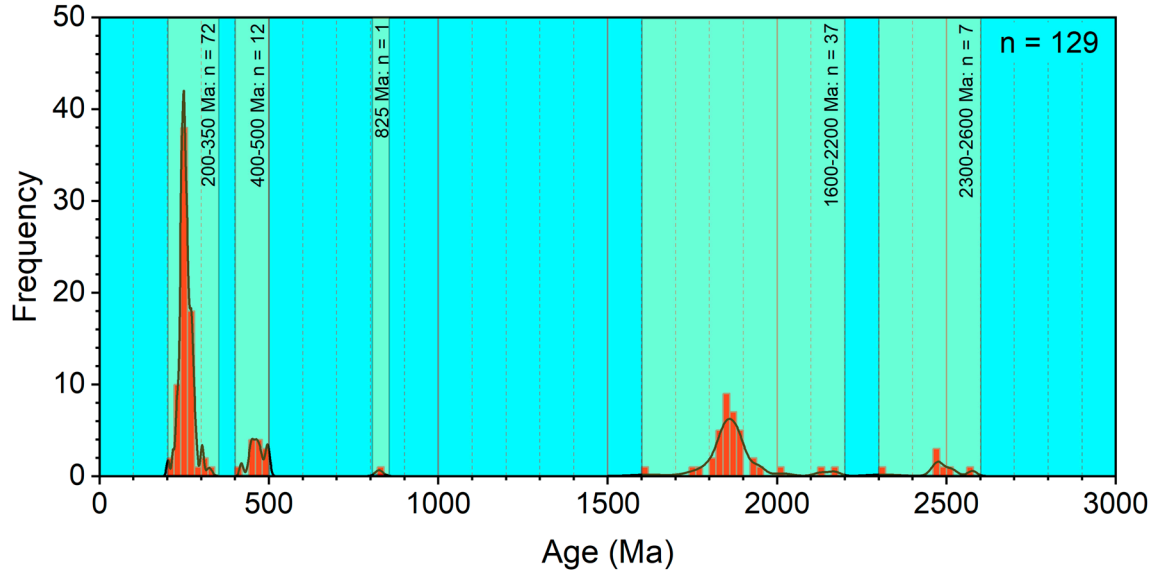

Fig. 5. Probability distribution diagrams and histogram of zircon ages in the samples.

reported weighted mean of low Th/U rim ages of Higo gneiss as 116.5 ± 18.7 Ma (95% conf.), and Maki *et al.* (2014) also reported weighted mean of low Th/U rim ages of metatexite migmatite in Higo gneiss as 116.0 ± 1.6 Ma (95% conf.). According to these data, it is virtually certain that metamorphism of the HMC occurred in ~116 Ma.

Acknowledgment

The author wishes to thank Dr. K. Yokoyama of the Ibaraki Nature Museum for helpful comments and editorial assistance on the preparation of the manuscript. Thanks are also due to Ms. Y. Kusaba for her help with SEM analysis and Dr. A. Murch for his English proof-reading. The author also thanks Prof. T. Komatsu of Kumamoto University for his help with sampling.

References

Chen, J. F., Xie, Z., Li, M. H., Zhang, X. D., Zhou, T. X., Park, Y. S., Ahn, K. S., Chen, D. G. and Zhang, X. (2003) U-Pb zircon ages for a collision-related K-rich complex at Shidao in the Sulu ultrahigh pressure terrane, China. *Geochemical Journal*, **37**: 35–46.

Cho, M., Kim, Y., and Ahn, J. (2007) Metamorphic Evolution of the Imjingang Belt, Korea: Implications for Permo-Triassic Collisional Orogeny. *International Geology Review*, **49**: 30–51.

Dickinson, W. R. and Gehrels, G. E. (2009) Use of U–Pb ages of detrital zircons to infer maximum depositional ages of strata: A test against a Colorado Plateau Mesozoic database. *Earth and Planetary Science Letters*, **288**: 115–125.

Hacker, B. R., Ratschbacher, L., Webb, L., Ireland, T., Walker, D. and Don, S. (1998) U-Pb zircon ages constrain the architecture of the ultrahigh-pressure Qinling–Dabie Orogen, China. *Earth and Planetary Science Letters*, **161**: 215–230.

Hamamoto, T., Osanai, Y. and Kagami, H. (1999) Sm–Nd, Rb–Sr and K–Ar geochronology of the Higo metamorphic terrane, west-central Kyushu, Japan. *Island Arc*, **8**: 323–334.

Horie, K., Takehara, M., Suda, Y. and Hidaka, H. (2013) Potential Mesozoic reference zircon from the Unazuki plutonic complex: geochronological and geochemical characterization. *Island Arc*, **22**: 292–305.

Horie, K., Tsutsumi, Y., Takeghara, M. and Higaka, H. (2018) Timing and duration of regional metamorphism in the Kagasawa and Unazuki areas, Hida metamorphic complex, southwest Japan. *Chemical Geology*, **484**: 148–167.

Hoshizumi, H., Ozaki, M., Miyazaki, K., Matsuura, H., Toshimutsu, S., Uto, K., Uchiumi, S., Komazawa, M., Hiroshima, T. and Sudo, S. (2004) *Geological map of Japan1:200000*, *Kumamoto*, Geological Survey of Japan, Tsukuba, Japan (in Japanese with English abstract).

Hoskin, P. W. & Black, L. P. 2000. Metamorphic zircon formation by solid-state recrystallization of protolith igneous zircon. *Journal of Metamorphic Geology*, **18**: 423–439.

Kinny, P. D., Wijbrans, J. R., Froude, D. O., Williams, I. S. and Compston, W. (1990) Age constraints on the geological evolution of the Narryer Gneiss Complex, Western Australia. *Australian Journal of Earth Sciences*, **37**: 51–69.

Liu, F. L., Gerdes, A., Liou, J. G., Xue, H. M. and Liang, F. H. (2006) SHRIMP U-Pb zircon dating from Sulu - Dabie dolomitic marble, eastern China: constraints on prograde, ultrahigh-pressure and retrograde metamorphic ages. *Journal of Metamorphic Geology*, **24**: 569–589.

Maki, K., Ishizaka, Y. and Nishiyama, T. (2004) Staurolite-bearing gneiss and re-examination of metamorphic zonal mapping of the Higo metamorphic terrane in the Kosa area, central Kyushu, Japan. *Journal of Mineralogical and Petrological Sciences*, **99**: 1–18.

Maki, K., Fukunaga, Y., Nishiyama, T. and Mori, Y. (2009) Prograde P-T path of medium-pressure granulite facies calc-silicate rocks, Higo metamorphic terrane, central Kyushu, Japan. *Journal of Metamorphic Geology*, **27**: 107–124.

Maki, K., Yui, T.-F., Miyazaki, K., Fukuyama, M., Wang, K.-L., Martens, U., Grove, M. and Liou, G. (2014) Petrogenesis of metatexite and diatexite migmatites determined using zircon U–Pb age, trace element and Hf isotope data, Higo metamorphic terrane, central Kyushu, Japan. *Journal of Metamorphic Geology*, **32**: 301–323.

Miyazaki, K. (2004) Low-P–high-T metamorphism and the role of heat transport by melt migration in the Higo Metamorphic Complex, Kyushu, Japan. *Journal of Metamorphic Geology*, **22**: 793–809.

Nagakawa, K., Obata, M. and Itaya, T. (1997) K-Ar ages of the Higo metamorphic belt. *Journal of the Geological Society of Japan*, **103**: 943–952 (in Japanese with English abstract).

Nakajima, T., Nagakawa, K., Obata, M. and Uchiumi, S. (1995) Rb-Sr and K-Ar ages of the Higo metamorphic rocks and related granitic rocks, Southwest Japan. *Journal of the Geological Society of Japan*, **101**: 615–620 (in Japanese with English abstract).

Obata, M., Yoshimura, Y., Nagakawa, K., Odawara, S. and Osanai, Y. (1994) Crustal anatexis and melt migrations in the Higo metamorphic terrane, west-central Kyushu, Kumamoto, Japan. *Lithos*, **32**: 135–147.

Osanai, Y., Hamamoto, T., Maishima, O. and Kagami, H. (1998) Sapphirine-bearing granulites and related high-temperature metamorphic rocks from the Higo metamorphic terrane, westcentral Kyushu, Japan. *Journal of Metamorphic Geology*, **16**: 53–66.

Osanai, Y., Kamei, A., Owada, M. and Hamamoto, T., (2001) Tectono-metamorphic evolution and related igneous activities of the Higo metamorphic terrane, west-central Kyushu, Japan. *Kyushu Tectonics Working Group News Letter*, **5**: 1–62 (in Japanese).

Osanai, Y., Masao, S. and Kagami, H. (1993) Rb–Sr whole

rock isochron ages of granitic rocks from the central Kyushu, Japan. *Memoirs of the Geological Society of Japan*, **42**: 135–150 (in Japanese with English abst).

Osanai, Y., Owada, M., Kamei, A., Hamamoto, T., Kagami, H., Toyoshima, T., Nakano, N. and Nam, T. N. (2006) The Higo metamorphic complex in Kyushu, Japan as the fragment of Permo–Triassic metamorphic complexes in East Asia. *Gondwana Research*, **9**: 152–166.

Paces, J. B. and Miller, J. D. (1993) Precise U-Pb age of Duluth Complex and related mafic intrusions, northern Minnesota: geochronological insights to physical, petrogenetic, paleomagnetic, and tectonomagmatic processes associated with the 1.1 Ga midcontinent rift system. *Journal of Geophysical Research*, **98**: 13997–14013.

Sakashima, T., Terada, K., Takeshita, T. and Sano, Y. (2003) Large-scale displacement along the Median Tectonic Line, Japan: evidence from SHRIMP zircon U-Pb dating of granites and gneisses from the South Kitakami and paleo-Ryoke belts. *Journal of Asian Earth Science*, **21**: 1019–1039.

Schiøtte, L., Compston, W. and Bridgwater, D. (1988) Late Archaean ages for the deposition of clastic sediments belonging to the Malene supracrustals, southern West Greenland: evidence from an ion probe U–Pb zircon study. *Earth and Planetary Science Letters*, **87**: 45–58.

Shibata, K. and Yamamoto, H. (1965) Pottasium–argon age determination on the Higo metamorphic rocks. *Bulletin of the Geological Survey of Japan*, **16**: 283–284.

Song, B., Nutman, A. P. Liu, D. and Wu, J. (1996) 3800 to 2500 Ma crustal evolution in the Anshan area of Liaoning Province, northeastern China. *Precambrian Research*, **78**, 79–94.

Stacey, J. S. and Kramers, J. D. (1975) Approximation of terrestrial lead isotope evolution by a two-stage model. *Earth and Planetary Science Letters*, **26**: 207–221.

Tsuji, S. (1967) Petrology of the Higo metamorphic complex in the Kosa-Hamamati Area, Kumamoto Prefecture, Kyushu. Japanese *Journal of Geology and Geography*, **38**:13–25.

Tsutsumi, Y., Horie, K., Sano, T., Miyawaki, R., Momma, K., Matsubara, S., Shigeoka, M. and Yokoyama, K. (2012) LA–ICP–MS and SHRIMP ages of zircons in chevkinite and monazite tuffs from the Boso Peninsula, Central Japan. *Bulletin of the National Museum of Nature and Science*, *Series C* **38**: 15–32.

Williams, I. S. and Claesson, S. (1987) Isotopic evidence for the Precambrian provenance and Caledonian metamorphism of high grade paragneisses from the Seve Nappes, Scandinavian Caledonides. *Contributions to Mineralogy and Petrology*, **97**: 205–217.

Williams, I. S. (1998) U–Th–Pb geochronology by ion microprobe. In: McKibben, M. A., Shanks, W. C. P. and Ridley, W. I. (Ed.), *Applications of Microanalytical Techniques to Understanding Mineralizing Processes. Reviews in Economic Geology 7*, Society of Economic Geologists, Littleton, CO. USA, pp. 1–35.

Wu, Y. B., Gao, S., Zhang, H. F., Yang, S. H., Jiao, W. F., Liu, Y. S. and Yuan, H. L. (2008) Timing of UHP metamorphism in the Hong'an area, western Dabie Mountains, China: evidence from zircon U–Pb age, trace element and Hf isotope composition. *Contribution to Mineralogy and Petrology*, **155**: 123–133.

Yamaguchi, M. and Minamishin, M. (1986) Metamorphic process and its correlation to the isotopic age of metamorphic rocks- example of the Higo metamorphic rocks. *Science reports*, *Department of Geology*, *Kyushu University*, **15**: 137–151 (in Japanese with English abstract).

Yamamoto, H. (1962) Plutonic and metamorphic rocks along the Usuki–Yatsushiro tectonic line in the western part of central Kyushu. *Bulletin of Fukuoka Gakugei University*, *Part III*, **12**: 93–172.

Yamamoto, H. (1983) Granulite facies rocks in the Higo metamorphic belt, Kumamoto Prefecture. *Bulletin of Fukuoka University of Education*, *Part III*, **33**: 73–85 (in Japanese with English abstract).